



# A pseudo-MT formulation for 3D CSEM inversion with a single transmitter

François Bretaudeau, Nicolas Coppo, Pierre Wawrzyniak, Sébastien Penz,  
Jean-François Girard

## ► To cite this version:

François Bretaudeau, Nicolas Coppo, Pierre Wawrzyniak, Sébastien Penz, Jean-François Girard. A pseudo-MT formulation for 3D CSEM inversion with a single transmitter. The 23rd Electromagnetic Induction Workshop - EMIW2016, Aug 2016, Chiang Mai, Thailand. p.248. hal-01328531

**HAL Id: hal-01328531**

**<https://hal-brgm.archives-ouvertes.fr/hal-01328531>**

Submitted on 8 Jun 2016

**HAL** is a multi-disciplinary open access archive for the deposit and dissemination of scientific research documents, whether they are published or not. The documents may come from teaching and research institutions in France or abroad, or from public or private research centers.

L'archive ouverte pluridisciplinaire **HAL**, est destinée au dépôt et à la diffusion de documents scientifiques de niveau recherche, publiés ou non, émanant des établissements d'enseignement et de recherche français ou étrangers, des laboratoires publics ou privés.

# A pseudo-MT formulation for 3D CSEM inversion with a single transmitter

F. Bretaudeau<sup>1,\*</sup>, N. Coppo<sup>1</sup>, P. Wawrzyniak<sup>1</sup>, S. Penz<sup>1</sup>, J-F. Girard<sup>2</sup>

<sup>1</sup> BRGM (French Geological Survey)

<sup>2</sup> EOST (CNRS & University of Strasbourg), formerly BRGM

\*Corresponding author, e-mail: f.bretaudeau@brgm.fr

**ABSTRACT:** Land EM methods provide useful information in domains such as geothermal energy, CO2 storage or water resources managements. However, the targets are usually close from urban areas where anthropogenic noise such as high power lines, industries and railways prevents from the use of Magnetotelluric (MT). Controlled-Source EM (CSEM) is thus generally preferred to MT. However, unlike for marine CSEM surveys used in oil prospection, logistical constraints on land surveys limit to the use of a few transmitters, usually 2 polarizations at a single position. Again due to noise constraints, it is usually preferred to place the transmitter close from the stations, which make impossible the use of CSAMT processing, as far field assumption is not respected. Thus the 3D inverse problem associated to this kind of survey suffers from very high sensitivity heterogeneities and singularities, in particular in the vicinity of the transmitter, that prevents from good convergence of the inversion process.

In order to achieve reliable local inversion with such pathologic sensitivities, several crucial aspects of the algorithm must be considered. Firstly, Gauss-Newton inversion must be preferred to a gradient-based method, and a very robust solver such as LSQR is necessary. Then a good parameterization must be chosen. Preconditioning of the system with model reparameterization must also be used to compensate for the sensitivity loss with depth. But we show that even with a Gauss-Newton resolution and efficient preconditioning of both data and model parameter, the inversion fails to converge to an accurate solution with single source position in cases where MT data inversion or CSEM with many transmitters provides successful results. In order to mitigate the sensitivity singularities, we propose to reformulate the CSEM inverse problem by recasting the data under the form of a pseudo-MT tensor. The associated sensitivities are a linear combination of the common CSEM sensitivities for electric and magnetic fields. We show on a synthetic model that this formulation highly reduces the footprint of the transmitter in the sensitivities even in the near field. It also provides a natural balance between the data and between the whole frequency range. Finally the approach allows the inversion to converge to a reliable result. This approach has been successfully applied on a 3D land survey in France with very complex geology, where the common CSEM inversion had provided biased results.

**KEYWORDS:** Land CSEM, 3D inversion, pseudo-MT tensor, model reparameterization, single transmitter.

## INTRODUCTION

Anthropogenic noise, cost and logistical constraints generally limit to the use of CSEM with a single transmitter position for the deep imaging of the electrical conductivity. As the inversion of CSEM data in the near field using a single transmitter position suffers from critical sensitivity singularities, we propose a robust inversion framework adapted to this ill-conditioned inversion problem. The framework relies specifically on a robust Gauss-Newton solver, several model parameter transformations to compensate for the heterogeneous sensitivities, and on the reformulation of the CSEM data under the form of a pseudo-MT tensor.

We first describe in the paper the approach used for modeling and inversion implemented in our code

POLYEM3D. Then we detail the new pseudo-MT formulation. In the last part of the paper, we illustrate its application on a pathologic synthetic case inspired from Grayver et al. (2013).

## METHODOLOGY

The POLYEM3D code used in this study relies on a hybrid EM modeling engine in the frequency domain with 1D semi-analytical modeling for a primary field in a 1D layered reference resistivity model and a finite-volume formulation on an irregular cartesian grid for the secondary field (Streich, 2009). Arbitrary sources such as long irregular wires can be considered through the semi-analytical formulation. The finite-volume formulation provides a linear system to be solved:

$$\mathbf{A}(\rho, \omega) \mathbf{E} = \mathbf{b}. \quad (1)$$

where  $\mathbf{A}$  is the finite-volume operator matrix,  $\rho$  a 3D resistivity distribution,  $\mathbf{E}$  the 3D electric field and  $\mathbf{b}$  the source term.

The computed data  $d_{s,r}^c$  (component  $c$  of the electric and/or magnetic field at each receiver  $r$  generated by the source  $s$ ) can be expressed as:

$$d_{s,r}^c = \wp_r^c \mathbf{E}_s \quad (2)$$

where  $\wp_r^c$  is a restriction operator that extract the value of the component of the field from the 3D electric field computed on the whole grid. It contains interpolation operators and curl operator for magnetic field.

Inversion of EM fields is achieved by minimising the misfit function:

$$\Phi = \Delta \mathbf{d}^\dagger \mathbf{W}_d^\dagger \mathbf{W}_d \Delta \mathbf{d} \quad (3)$$

with  $\Delta \mathbf{d} = \mathbf{d}_{\text{obs}} - \mathbf{d}_{\text{cal}}$  the data residual vector. In CSEM inversion the data vectors usually contains each component of the electric and/or magnetic fields for each station of the survey, each source and each frequencies. However, different kind of observable can be used to build the data vector, for example amplitudes, phases, maximum of the polarization ellipses, angles, or any kind of representation of the data. In the framework of local linear inversion, we want at each iteration to determine the model update  $\Delta \mathbf{m}$  solution of the Gauss-Newton equation:

$$\text{Re}(\mathbf{J}^\dagger \mathbf{J}) \Delta \mathbf{m} = -\text{Re}(\mathbf{J}^\dagger \mathbf{W}_d \Delta \mathbf{d}) \quad (4)$$

where  $\mathbf{J}$  is the sensitivity matrix.

### Reparameterization of the problem

The sensitivity  $\mathbf{J}$  is proportional to the electric field, and thus decreases rapidly with depth and with the distance from the source, resulting in a very poorly conditioned linear system to be solved. In POLYEM3D, this linear system is solved with LSQR that is known to be efficient for poorly conditioned linear system. Furthermore, preconditionning can be applied by model reparameterization. Instead of performing inversion of  $\rho$ , we can inverse  $\mathbf{m}$ :

$$\mathbf{m} = \mathbf{G}^{-1} \mathbf{D}^{-1} C(\rho) \quad (5)$$

with  $C$  a change of variable (such as logarithm),  $D$  a linear operator that rescale the sensitivity loss with depth (such as in Plessix & Mulder (2008)), and  $G$  a linear operator that change the basis of description of the model (for instance a basis of splines described on

a coarse grid). Each line of the sensitivity matrix thus can be written:

$$\mathbf{J}_{s,r}^c = \mathbf{G}^t \mathbf{D}^t \frac{1}{C'(\rho)} \mathbf{E}_s \frac{\partial \mathbf{A}}{\partial \rho} \mathbf{A}^{-1} \wp_r^{ct} \quad (6)$$

### A pseudo-MT formulation

The reparameterization allows to perform efficient 3D inversion for MT or multiple source CSEM. However it is still not enough to inverse CSEM data when a single source is used, as the sensitivity singularity at the source cumulates over each line of  $\mathbf{J}$ . We found that recasting the data acquired with two different transmitters using a MT tensor formulation mitigates the singularity due to the transmitter both in the data and in the sensitivities. Taking for a station the definition of a  $Z$  tensor as a transfer function:

$$\begin{pmatrix} E^x \\ E^y \end{pmatrix} = \begin{bmatrix} Z_{xx} & Z_{xy} \\ Z_{yx} & Z_{yy} \end{bmatrix} \begin{pmatrix} H^x \\ H^y \end{pmatrix}, \quad (7)$$

and considering two different sources (it can be typically two polarization of a single transmitter), we can obtain for each station the 4 components of this pseudo-MT tensor by a combination of the 8 electric and magnetic fields generated by those two sources:

$$Z_{ij} = f(E_s^c, H_s^c). \quad (8)$$

Recasting the CSEM data under this form reduce the number of data by 2 and results in a sensitivity matrix that is a linear combination of the common CSEM sensitivities weighted by the values of the fields:

$$J_{Z_{ij}} = f(J_{E_s^c}, J_{H_s^c}, E_s^c, H_s^c) \quad (9)$$

The pseudo-MT tensor is not to be linked to an apparent resistivity or a MT tensor because depending on the frequency and the source-receiver distance considered, the far field condition is not always respected. It is however a well balanced observable that can be inverted if an accurate modeling of the real transmitters is considered.

### APPLICATION ON A SYNTHETIC CASE

We illustrate the behavior of the new formulation on a 3D synthetic resistivity inspired from the model of Grayver et al. (2013) represented figures 1 and 3. The survey is composed of 100 stations over a  $5\Omega.m$  medium with 3 anomalies at  $1\Omega.m$ ,  $50\Omega.m$  et  $100\Omega.m$ . We consider the inversion of MT data (far field), and inversion of CSEM data generated with two orthogonal polarization located at 2km from the closest station, and 5 frequencies from 32s to

16Hz. The CSEM data are inverted first using both normalized electric and magnetic fields, and then using the pseudo-MTtensor formulation.

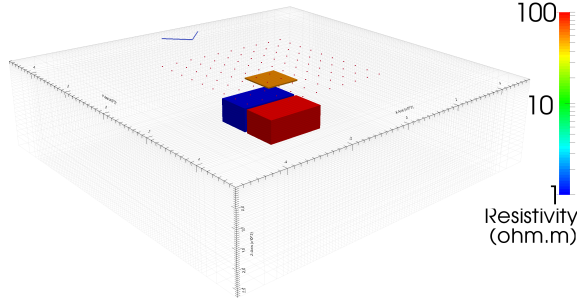


**Figure 1** Resistivity and acquisition model taken from Grayver et al. (2013)

The figure 2 represents the gradient of the cost function at 32s (i.e.  $\text{Re}(\mathbf{J}^\dagger \Delta \mathbf{d})$ ) without the reparameterizations described above and no regularization, for the MT data, for the CSEM data using weights in  $\mathbf{W}_d$  to normalize the data, and for the CSEM data with the pseudo-MT tensor formulation. At 32s the skin depth is 6.4km so the CSEM survey is such we are clearly not in far field.

With the MT data, the gradient shows as expected sensitivity to both anomalies and a maximum of sensitivity just above the station array. With the CSEM data, when weighed fields are inverted, the gradient shows small sensitivities just above the station array but a very high sensitivity zone close to the transmitter position. The sensitivity cumulates under the transmitter and spreads out above the station array. This effect is very pronounced here due to the unbalance between the number of transmitters and the number of stations. The phenomenon is not visible with MT data for which sources are supposed to be far from the array, and is not so critical for multiple source CSEM, as in Grayver et al. (2013) or Plessix & Mulder (2008), because the maximum of sensitivity at the source location spreads out all along the survey. The last picture in figure 2 shows that using a pseudo-MT tensor formulation, the sensitivity anomaly under the transmitter is reduced and is closer from the MT sensitivity even though we are not in far field. This behavior is also observed in far field.

The footprint of the transmitter in the sensitivity is not completely removed but is reduced enough to allow convergence of the inversion. We show in figures 3 to 6 the inversion result obtained for MT

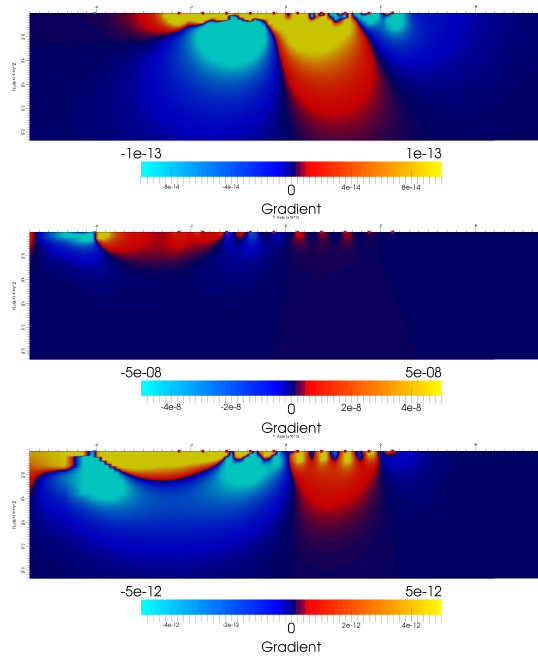


**Figure 2** Profile of the gradient of the cost function computed for the 1st frequency (32s) for (a) MT data. (b) CSEM with normalized data. (c) CSEM with pseudo-MT tensor formulation.

data, CSEM data with weighed data and pseudo-MT tensor formulation using 5 frequencies (32s, 8s, 1Hz, 4Hz and 16Hz). The station array is in far field condition for the highest frequencies, near field for the lowest, and intermediate in between. Sharper results should be obtained with more efficient regularization but the conclusions should not differ. Even though the deep resistive anomaly is underestimated and a few artefacts appear around the shallow anomaly, the MT data inversion reconstructs quite well the 3 anomalies in very few iterations ( $< 20$  iterations). The inversion of CSEM weighted data fails to converge. It gets stuck in a local minimum after the 1st iteration. We clearly see in the inverted model the footprint of the transmitter sensitivity anomaly that dominates the reconstruction. The deep anomalies are shifted and smoothed along the wavepath between the sources and the stations. The shallow anomaly is not reconstructed, and several artefacts appear close to the surface. Using the pseudo-MT tensor formulation, artefacts are still visible under the transmitter, but the deep anomalies are better reconstructed and the shallow anomaly is well imaged. Convergence is also better (15 iterations).

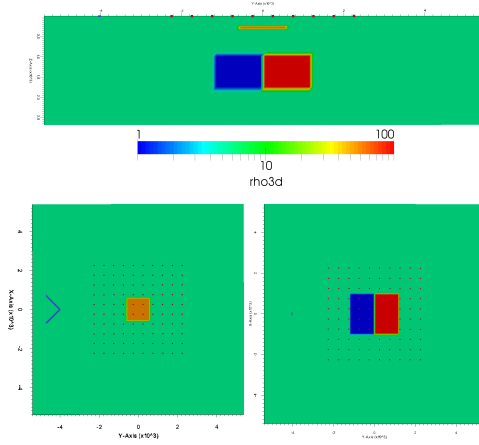


**Figure 3** Exact resistivity model with 3 anomalies, 100 station and 2 orthogonal transmitters (a) (yz) profile (b) top view at 280m. (c) top view at 1000m.

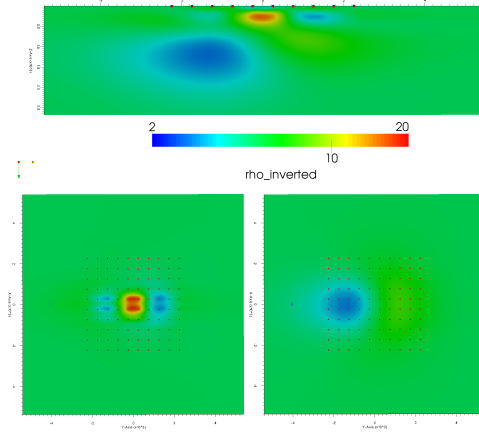


**Figure 4** Final inverted result for the MT data. (a) (yz) profile (b) top view at 280m. (c) top view at 1000m.

## CONCLUSIONS

We proposed an alternative formulation of the CSEM inversion problem by recasting data as a pseudo-MT tensor. We show on a synthetic case that this formulation, when used with an accurate Gauss-Newton inversion and an efficient reparameterization allows to perform 3D inversion of CSEM land data using a single transmitter where common approach fails.

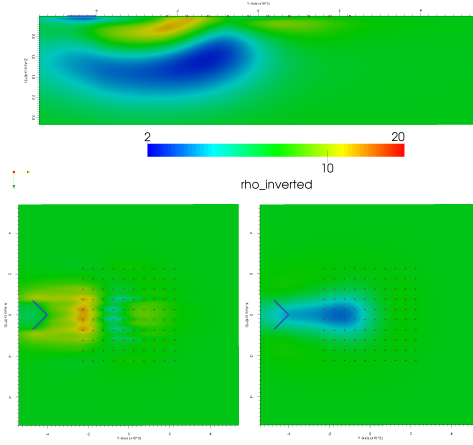


**Figure 5** Final inverted result for the CSEM data with normalized fields. (a) (yz) profile (b) top view at 280m. (c) top view at 1000m.

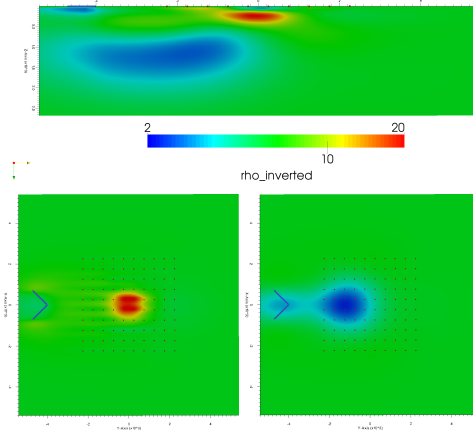


**Figure 6** Final inverted result for the CSEM data with the pseudo-MT tensor formulation. (a) (yz) profile (b) top view at 280m. (c) top view at 1000m.

## REFERENCES

- Grayver, A., Streich, R., & Ritter, O., 2013. Three-dimensional parallel distributed inversion of csem data using a direct forward solver., *Geophysical Journal International*, **193**, 1432–1446.
- Plessix, R. & Mulder, W., 2008. Resistivity imaging with controlled-source electromagnetic data: depth and data weighing., *Inverse Problem*, **24**, 034012.
- Streich, R., 2009. 3d finite-difference frequency-domain modeling of controlled-source electromagnetic data: Direct solution and optimization for high accuracy., *Geophysics*, **74**(5), F95–F105.